

## PHASE COMPOSITION AND MICROMORPHOLOGY OF POLYPHASE DIOPSIDE-BEARING MATERIALS

Momchil Dyulgerov<sup>1</sup>, Bojidar Jivov<sup>2</sup>, Vladimir Petkov<sup>2</sup>,  
Mihaela Aleksandrova<sup>2</sup>, Gabriel Peev<sup>2</sup>

<sup>1</sup>Department of Mineralogy, Petrology and Economic Geology  
Faculty of Geology and Geography, Sofia University "St. Kliment Ohridski"  
15 Tsar Osvoboditel Blvd., Sofia 1504  
Bulgaria, momchil@gea.uni-sofia.bg (M.D.)

<sup>2</sup>Bulgarian Academy of Sciences  
Institute of Metal Science, Equipment and Technologies  
with Hydro - and Aerodynamics Centre "Acad. A. Balevski"  
67 "Shipchenski Prohod" Blvd., Sofia 1574  
Bulgaria, b\_jiv@abv.bg (B.J.); vladimir2pe@yahoo.com (V.P.);  
mihaela.krasimirova@mail.bg (M.A.); gabi.peev67@gmail.com (G.P.).

Received 18 March 2025

Accepted 07 May 2025

DOI: 10.59957/jctm.v60.i5.2025.6

---

### ABSTRACT

*Based on natural carbonate raw materials, oxide components and fluorite, polyphase materials with a silicate composition were synthesized in laboratory conditions. The phase composition, structure and micromorphology of the obtained experimental samples were studied. Their textural properties - medium to micro - grained, spinifex or chilled marginal zones, attest that they have crystallized from a melt. In separate areas, gradual transitions from one type of texture to another and a limited presence of amorphous zones were observed. The diopside is the main phase that appear in all samples as prismatic to needle - shaped crystals. Fluorite presents in small amount in all samples with spheroidal to irregular shape. Wollastonite, akermanite, calcite and quartz also present as important phases according to sample's composition. Zincian hydroxide, chromite and an unidentified pigment are small constituents and reflect addition of various metals as colorants.*

*Keywords: silicate melt, polyphase materials, diopside.*

---

### INTRODUCTION

Modern silicate technologies allow the production of a significant variety of traditional, standard, innovative and high - tech products with diverse performance properties and wide application [1 - 5]. The production activity of the silicate industry is carried out through various technological methods that provide for the use of specialized equipment, raw materials subjected to standard incoming control, optimal batch compositions, highly efficient moulding methods, cost - effective and controlled process of thermal treatment of the compositions to irreversible formation of monophasic or polyphasic products with the necessary target

properties [6, 7]. The technological process allows the production of durable, non - flammable, water - resistant materials with appropriate mechanical, physicochemical, thermal, optical and other indicators [5, 8]. The resulting separate categories of products with diverse functional characteristics find use in various fields: mechanical engineering, instrument making, metallurgy, optics, electronics, energy, implantology and many others [1 - 3, 9 - 11].

In modern construction, silicate materials are widely used in the construction of durable load - bearing structures, external enclosing elements of buildings, internal partition walls, flooring, cladding elements and several others [12, 13]. There is a wide range of building

ceramics, glass products, glass - ceramic materials, sanitary ware, inorganic hydraulic binders (Portland cement), and others [4, 12 - 15].

Various silicate materials are applicable for equipping industrial facilities (furnaces and others) and installations specialized for performing production activities in conditions of specific, high - temperature or aggressive environments [6].

Due to the proven high - performance properties of silicate products and their importance for various technical fields, the development of innovative functional materials based on silicate phases is of current interest. In this regard, the technological possibilities for the synthesis of diopside - containing materials with different structures and characteristics have been studied: glass - ceramics [16 - 18], ceramic materials [19 - 24], pigments [25, 26] and others. Various precursor - natural raw materials, industrial waste products or high - purity reagents are used. Several technological approaches have been applied to prepare the experimental samples: solid - phase synthesis, melt crystallization, hydrothermal method, sol - gel technology, glass crystallization, and others [21, 22].

The choice of diopside is consistent with the crystallochemical specificity of the minerals of the pyroxene group, which form series of solid solutions with complete or limited isomorphic substitution [23, 25, 26]. Experimental samples were synthesized in the system  $\text{CaO} - \text{MgO} - \text{SiO}_2 - (\text{RO or } \text{R}_2\text{O}_3)$ , where calcium and magnesium can be partially replaced by chromophore components. Ceramic pigments based on diopside were obtained by using traditional raw materials and doping with various chromophore elements (transition and rare earth metals). The mechanism of isomorphic substitution of the chromophore in the structure of the dominant phase was studied. Analyse dare correlation dependencies composition -structure - properties of the developed diopside materials and the optimal technological conditions of synthesis have been determined. The effect from the introduction of chromophore impurities is determined by several factors: specificity of the chromophore, concentration, spatial distribution, valence state, ionic radius, crystallographic position, characteristics of the main phase, presence and ratio of other phases, technological parameters of the synthesis and others.

At the same time, the synthesis of materials with a

phase composition formed by the co - presence of diopside and other phases (combining their characteristics) allows the production of materials with diverse indicators.

The aim of this work is to study the phase composition, structure and micromorphology of polycrystalline samples with a dominant diopside content obtained from a melt based on sedimentary carbonate raw materials, quartz sand and other components. The role of the introduced modifying additives on the phase formation processes was monitored. According to the established structural characteristics and phase composition, the existing prospects for the preparation of functional products and potential application of the obtained materials have been analysed.

## EXPERIMENTAL

When preparing the experimental samples, standard laboratory equipment was used: precision balance model RSV 200 - 2 KERN, analytical balance Sartorius MSU225P, standard platform scale up to 10 kg, porcelain ball mill with a working volume of 50 L (rotation speed about  $260 \text{ rev min}^{-1}$ ), laboratory dryer Astel, a set of standard laboratory sieves, an agate mortar, a metal matrix, corundum crucibles, laboratory baths and more.

The thermal treatment of the prepared experimental compositions was carried out in a laboratory programmable Netzsch muffle furnace, equipped with an electronic programmer, allowing controlled change and maintenance of the parameters of the optimal temperature regime: rate of temperature increase and decrease, isothermal holds, maximum temperature, and others.

In the prepared experimental compositions (in wt %), dolomite, quartz sand, limestone,  $\text{CaF}_2$  and were used. In the different batches  $\text{ZnO}$ ,  $\text{CoO}$ ,  $\text{Cr}_2\text{O}_3$ ,  $\text{TiO}_2$  and  $\text{Fe}_2\text{O}_3$  were introduced as modifying additives.

Nominal composition number 1: dolomite - 46, limestone - 14, quartz sand - 30,  $\text{CaF}_2$  - 3,  $\text{ZnO}$  - 6,  $\text{CoO}$  - 1.

Nominal composition number 2: dolomite - 43, limestone - 10, quartz sand - 33,  $\text{CaF}_2$  - 5,  $\text{Cr}_2\text{O}_3$  - 3,  $\text{TiO}_2$  - 2,  $\text{Fe}_2\text{O}_3$  - 4,

Nominal composition number 3: dolomite - 40, limestone - 6, quartz sand - 36,  $\text{CaF}_2$  - 8,  $\text{ZnO}$  - 8,  $\text{Fe}_2\text{O}_3$  - 2.

At the same time, the use of some natural raw materials is

accompanied by the introduction of additional impurities into the compositions.

The provided quantities of natural raw materials were subjected to grinding (for 12 h), drying at 150°C (for 24 h) and sieving to the required fractional composition (0.051 - 0.09 mm). After weighing, mixing and homogenizing the reagents, a series of batches was prepared. The prepared batch compositions were placed in corundum crucibles and subjected to heat treatment in the furnace until a melt was formed. The heat treatment of the compositions was carried out in an air environment by applying a developed temperature regime, providing a heating rate of 5°C min<sup>-1</sup> and a series of isothermal holds: 300°C (30 min), 600°C (20 min), 900°C (20 min), 1000°C (20 min) and a maximum temperature of about 1460°C (20 min). By pouring the formed melt into a metal matrix and free smoothing, experimental monolithic specimens were obtained.

The powder XRD patterns were recorded on a Bruker D8 Advance diffractometer. Filtered Co - K $\alpha$  radiation was used in the range 2 $\theta$  4 - 80°, step 0.02° 2  $\theta$ , and exposure time per step 1.5 s. The specialized software Diffrac.Eva was used for qualitative and semi-quantitative phase composition determination.

Microscopic preparations were prepared from the obtained test samples in laboratory conditions. Optical investigations were performed on a Leica 7715 microscope equipped with a camera for microphotographs. Whole - rock chemistry of major oxides and some trace elements were obtained by XRF Epsilon3 XLE (Panalytical). The polarized Raman spectra were obtained on a micro - Raman spectrometer LabRam (Horiba Jobin - Yvon) under 632.8 nm excitation from a He - Ne laser. The laser radiation was focused in a spot with diameter ~ 2  $\mu$ m by an x100 Olympus microscope objective on the selected oriented crystals.

A modernized Amsler loading test machine was used in the mechanical tests. The loading of the samples was carried out between flat - surfaced tips made of hardened tool steel and an applied loading speed up to 0.8 mm s<sup>-1</sup> and a maximum loading range tailored to the specific test samples.

The microhardness of the test specimens was determined by the Vickers method using an apparatus consisting of a stage and an eyepiece - micrometre. The apparatus is equipped with a diamond indenter (with a square base and an angle between the sides of 136°) on which a load of 100 g is exerted for 5 s.

## RESULTS AND DISCUSSION

Monolithic experimental samples with a dominant diopside content and the presence of other phases were obtained in laboratory conditions.

The X - ray phase analysis (Fig. 1) of sample number 1 registered the presence of diopside, wollastonite, zinc hydroxide, and fluorite.

The fabric of the sample is massive, with no orientation of crystallized phases (Fig. 2). The texture is fine - equal grained; in the marginal zones observe micro - grained; spherulitic texture with radial diopside also appears. Glassy texture in chilled zones is rare. The transition from fine grained to amorphous zones is rapid, in the range of 10 - 30  $\mu$ m. These glassy zones are centred around voids in the sample and could be interpreted as zones of degassing and consequent rapid cooling and annealing of the melt.

The diopside is the main phase and forms several aggregate types. The dominant one is prismatic crystals; the tabular ones are less common. Toward the margins of the sample spinifex and spherulitic textures become common, needle like crystals with wavy structure also appear, comb - like structures are less typical.

Wollastonite is platy to lamellar and hardly distinguishable from diopside. Apart from XRD patterns, only its negative optical sign permits proper identification of wollastonite. Fluorite appears as small, oval or irregular aggregates, it is colourless and with low relief.

Through the X - ray phase analysis (Fig. 3) of sample number 2, the following have been identified diopside, calcite, fluorite, akermanite, and chromite.

Several texture types present in the sample (Fig. 4 and 5). The central part possesses even and medium grained texture with diopside crystals in the range 100 - 300  $\mu$ m and spheroidal voids with diameter 50 - 200  $\mu$ m, partially filled by fluorite and probably by calcite. In the periphery of the sample with rapid transition the texture changes as evidence for fast cooling and crystallization appear: the acicular diopside crystals show subparallel disposition (spinifex texture) oriented perpendicular to the solidification front; spherulitic and comb - like textures also present. In the marginal zones the texture becomes micro - grained with crystals up to 10  $\mu$ m. The transition from medium to micro grained textures is rapid, in the range of 100  $\mu$ m. Variable voids present in the sample: their shapes are spheroidal to completely irregular.

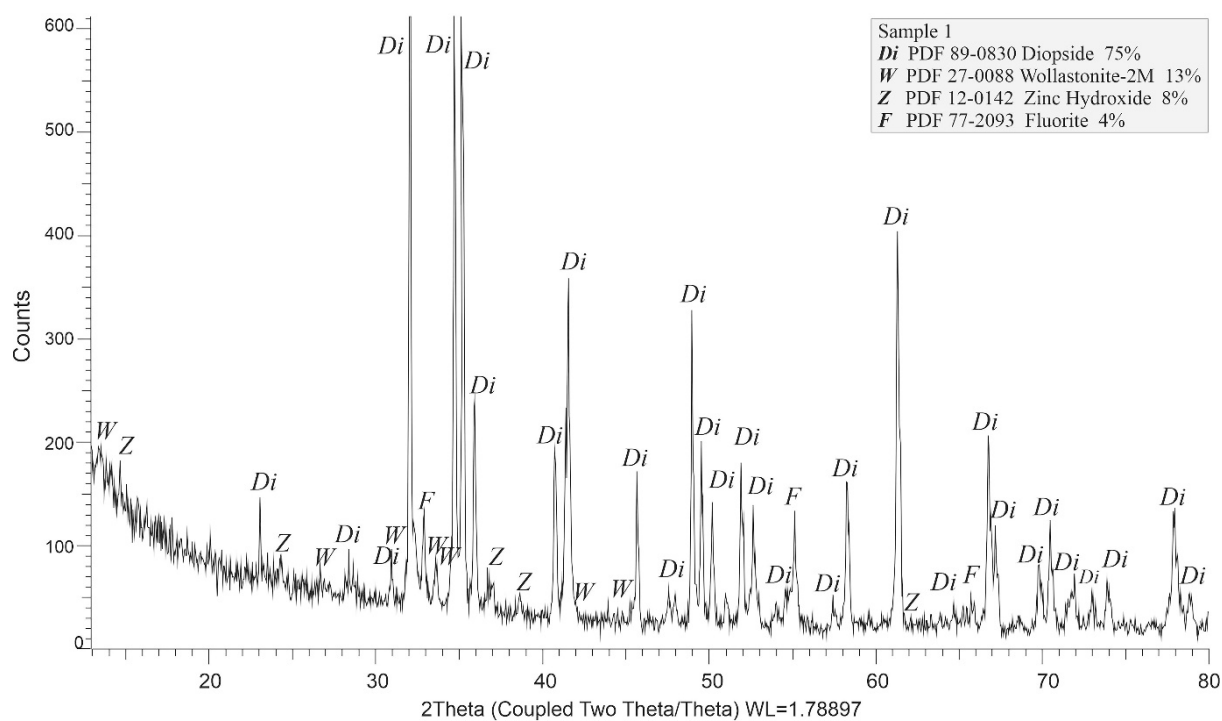


Fig. 1. X - ray phase analysis of sample number 1.

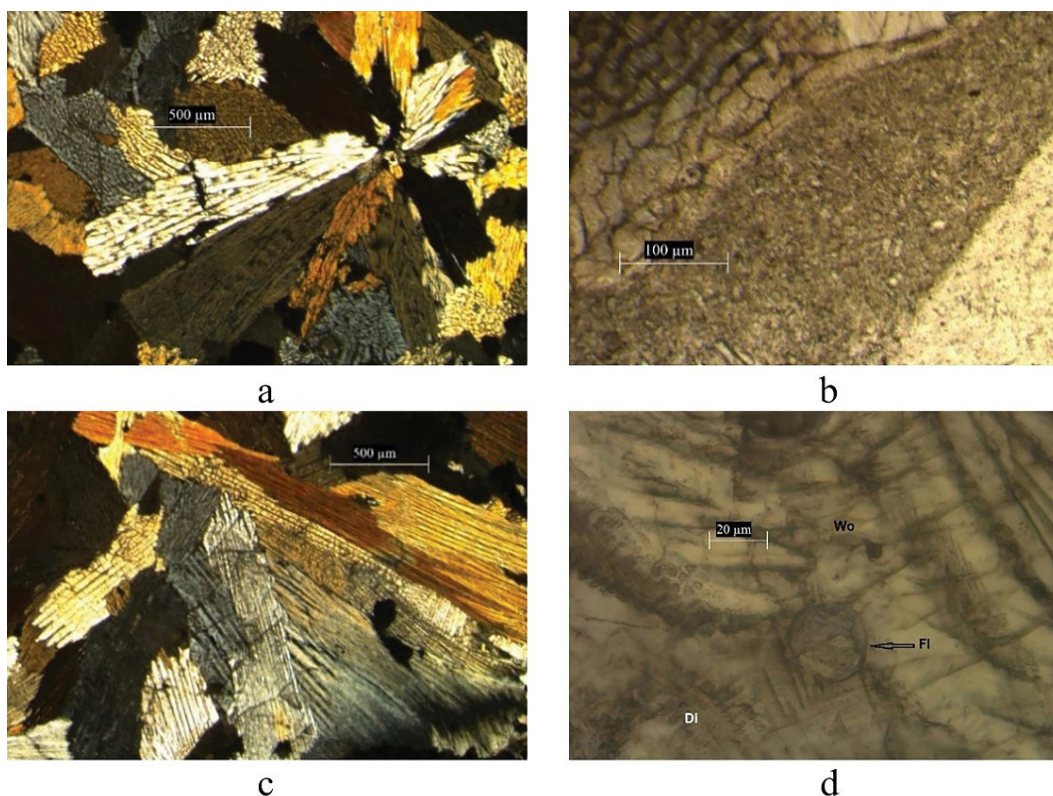


Fig. 2. Photomicrographs of sample 1: (a) - Prismatic diopside crystals with spherulitic texture (crossed nicols); (b) - Transition from fine grained to glassy texture (parallel nicols); (c) - Spinifex structure and wavy character of diopside crystals (crossed nicols); (d) - Fluorite (Fl), wollastonite (Wo) and diopside (Di) (parallel nicols).



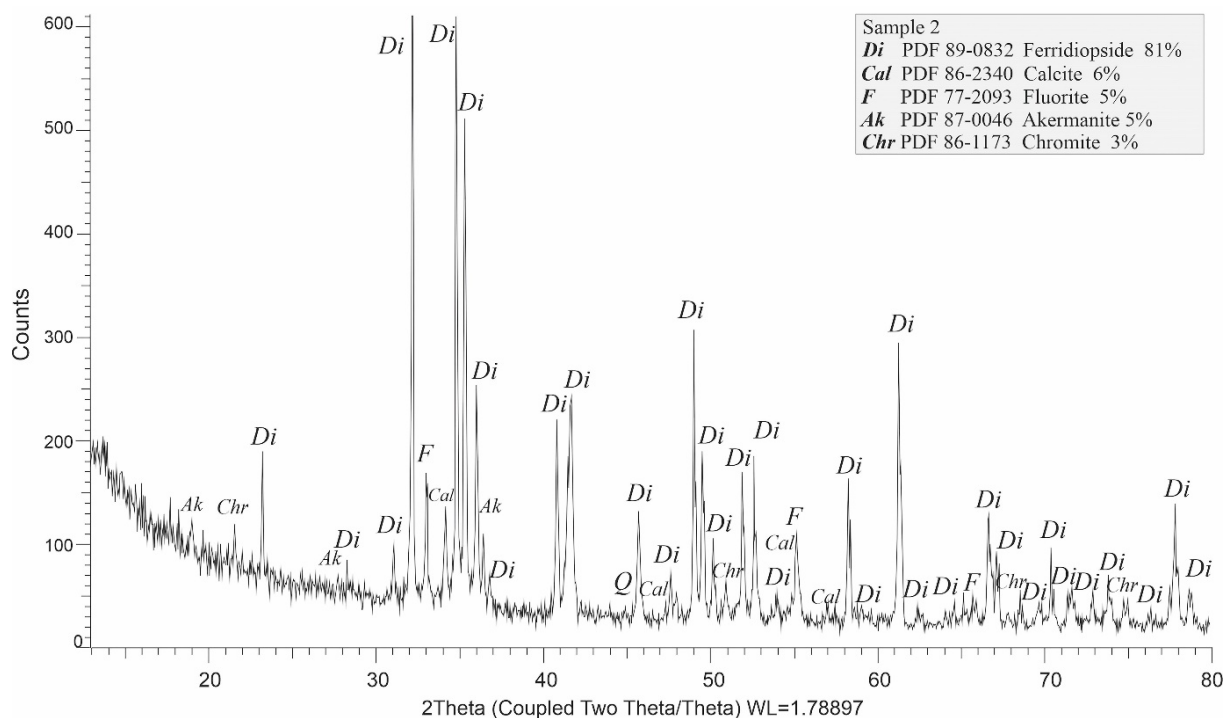


Fig. 3. X - ray phase analysis of sample number 2.

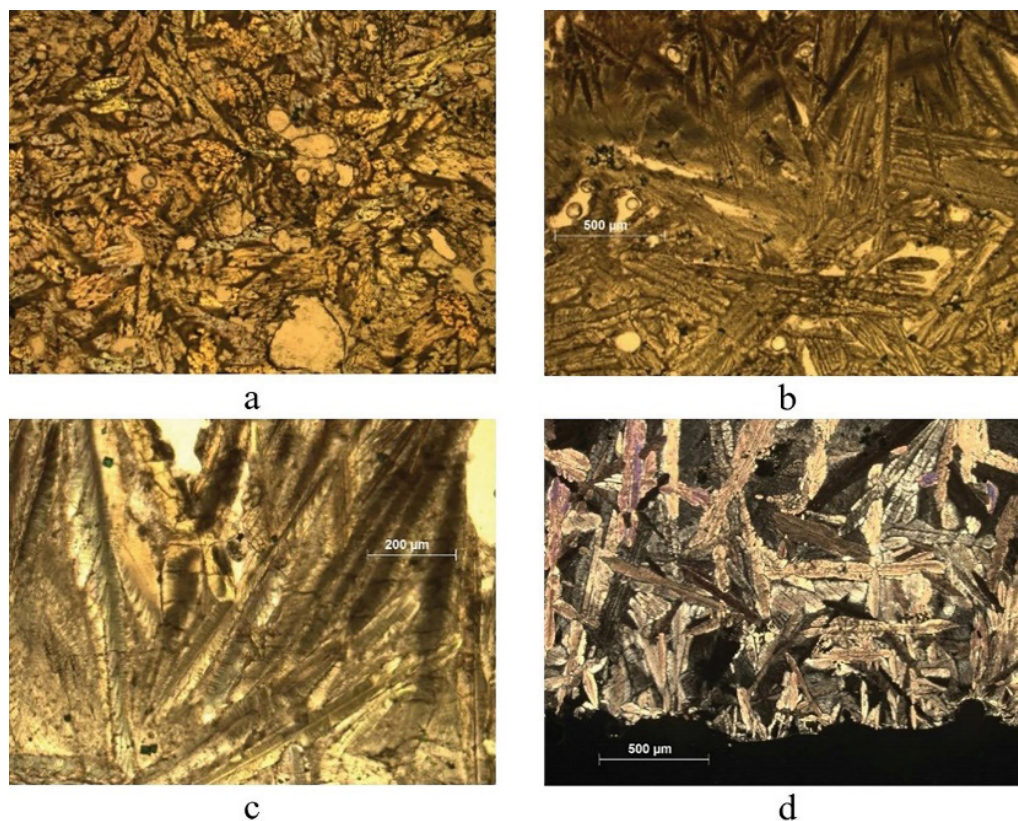


Fig. 4. Photomicrographs of sample 2: (a) - Central parts of the sample with even and medium grained texture and diopside crystals (parallel nicols); (b) - Transition from fine and even grained texture (down) to the zone of fast cooling, evidenced by the presence of acicular crystals and comb-like texture (upper part) (parallel nicols); (c) - Subparallel orientation of diopside (spinifex texture) (parallel nicols); (d) - Micrograined texture at the end of the sample (parallel nicols).

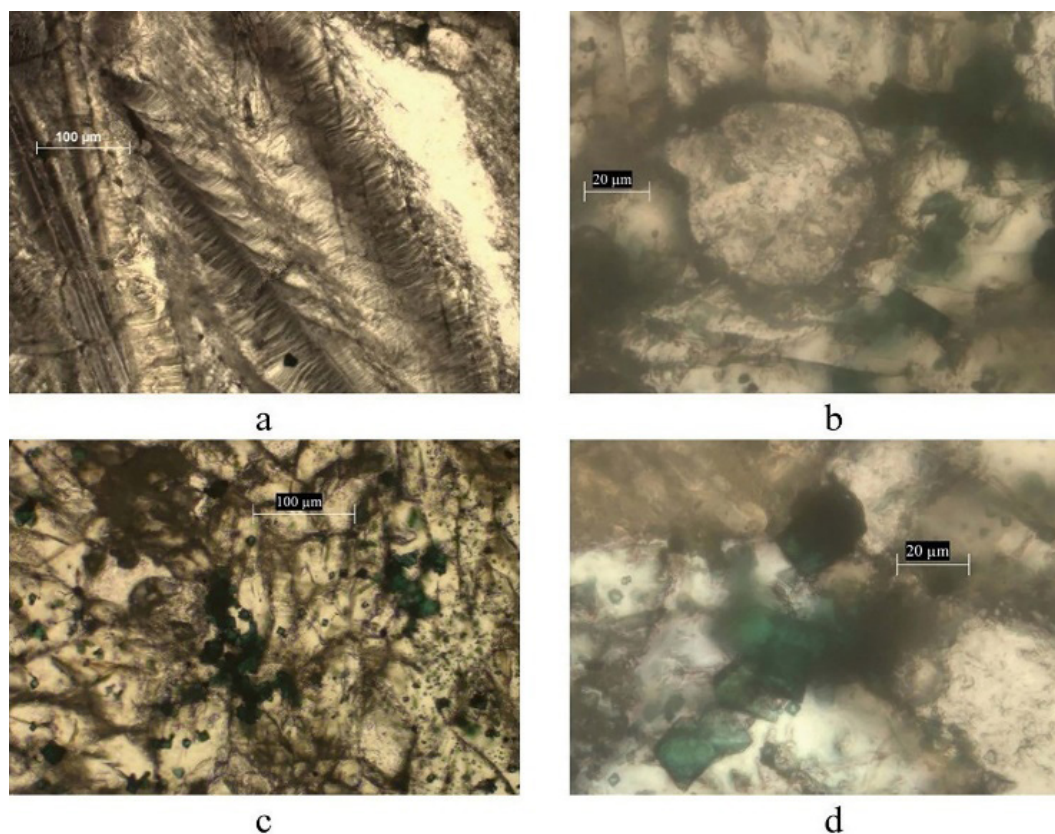


Fig. 5. Photomicrographs of samples 2 (all with parallel nicols): (a) - Comb - like texture of diopside in the annealing zone (parallel nicols); (b) - Fluorite (in the center), chromite (black) and unspecified chromate phases (green); (c) - Chromite (dark) and chromate crystals (green); (d) - Chromite (dark) and chromate crystals (green).

The main phase in the sample is diopside. It appears as stubby prismatic or platy to acicular crystals. Diopside displays moderate relief and birefringence from the end of second and the beginning of third order. Akermanite is rare and virtually indistinguishable from diopside. It forms transparent and platy crystal with low birefringence and uniaxial optical signal. Fluorite is rare and forms irregular to spherical aggregates partially filling cavities and voids. It is unclear whether this is primarily characteristic of the sample, or it is acquired during the preparation of the sample.

XRD study showed the presence of chromite, but the microscope observations revealed that at least two compositionally similar phases are present. The opaque one is with quadratic to oval crystals, isotropic in reflected light and corresponds to chromite. The more widespread phase is greenish, transparent and anisotropic, with strong relief and high birefringence. It forms quadratic, rectangular or irregular crystals or

it is rimmed on chromite. The close appearance of the chromite and the greenish phase is evidence that they have a close resemblance. The colour and anisotropic optical properties suggest that this phase is chromate ( $\text{CrO}_4^{2-}$ ), most probably Zn and / or Co bearing. As both  $\text{ZnCrO}_4$  and  $\text{CoCrO}_4$  are strong pigments we consider that this compound is responsible for the greenish colour of the sample.

XRD revealed the presence of carbonate phase (probably calcite) that we cannot confirm with microscope investigation. A possible explanation is that carbonate was scrubbed during polishing of the sample (as being with low hardness) or XRD patterns belong to another phase.

The X - ray phase analysis (Fig. 6) of sample number 3 registered the presence of diopside, fluorite, zinc hydroxide, and quartz.

The fabric of the sample is massive, with no orientation of crystallized phases (Fig. 7 and 8). The



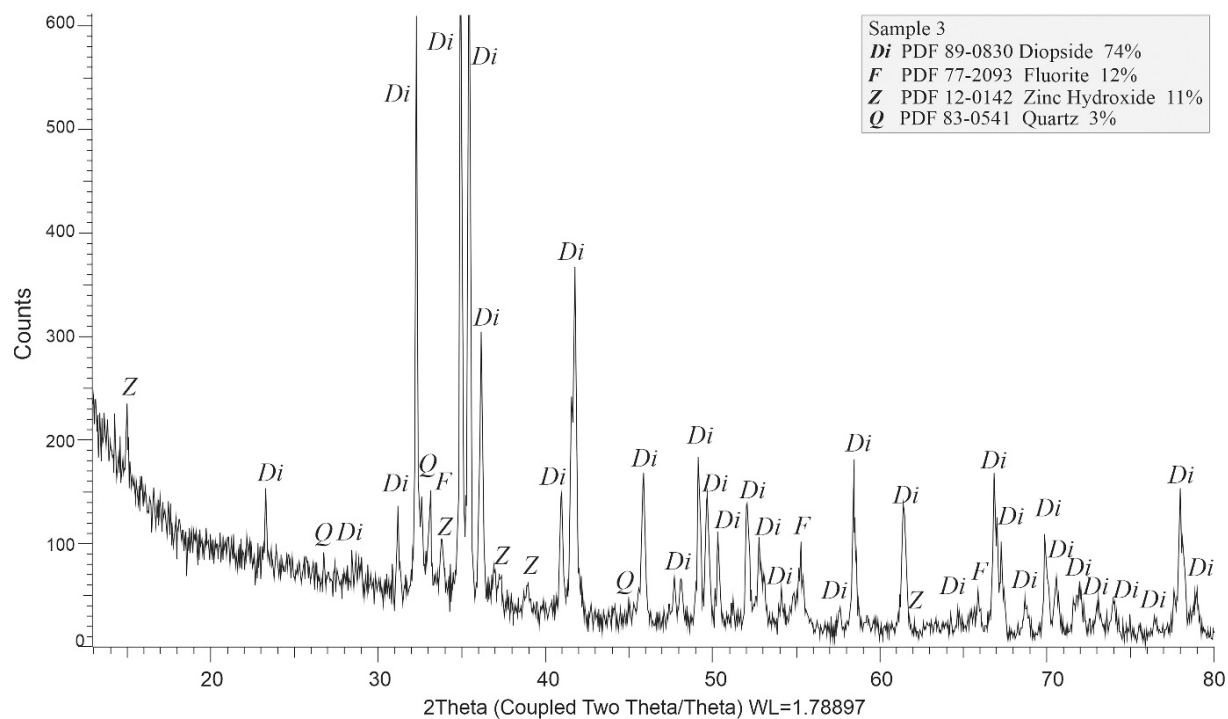


Fig. 6. X - ray phase analysis of sample number 3.

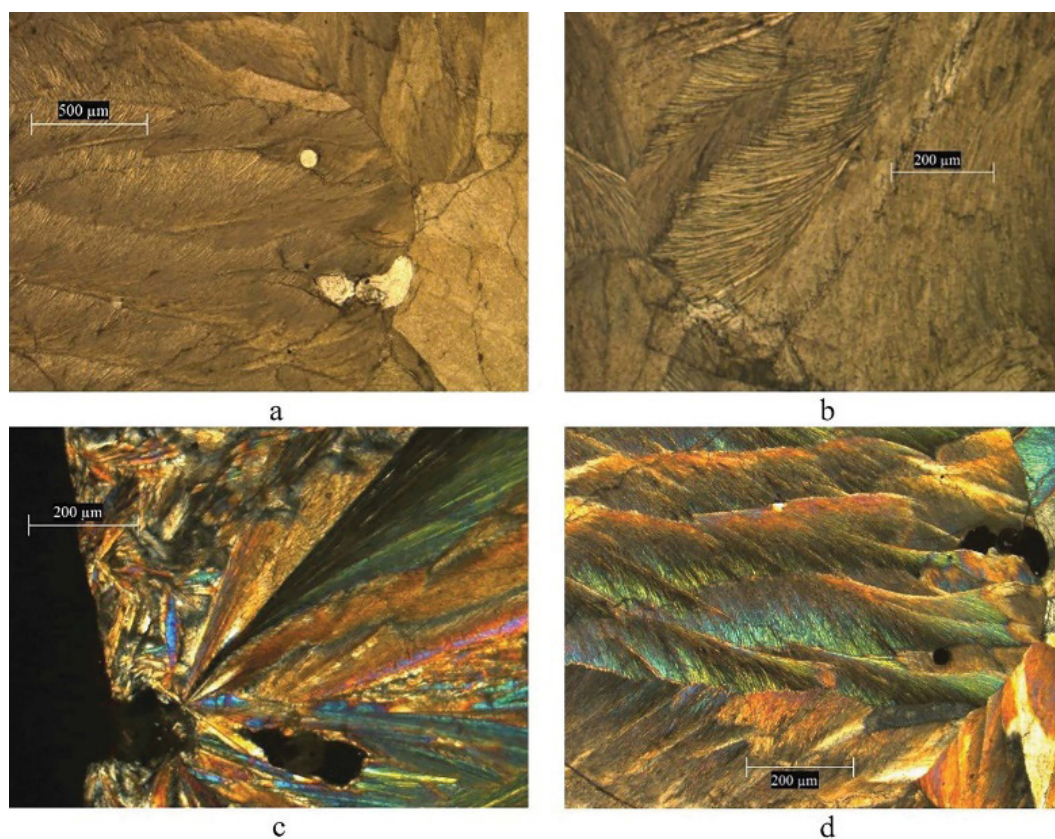


Fig. 7. Photomicrographs of sample 3: (a) - Massive fabrics with oval or elliptical voids (parallel nicols); (b) - Needle - like diopside with spinifex texture (parallel nicols); (c) - Annealing zone with fine grained diopside and abundant voids (crossed nicols); (d) - Wavy diopside (crossed nicols).

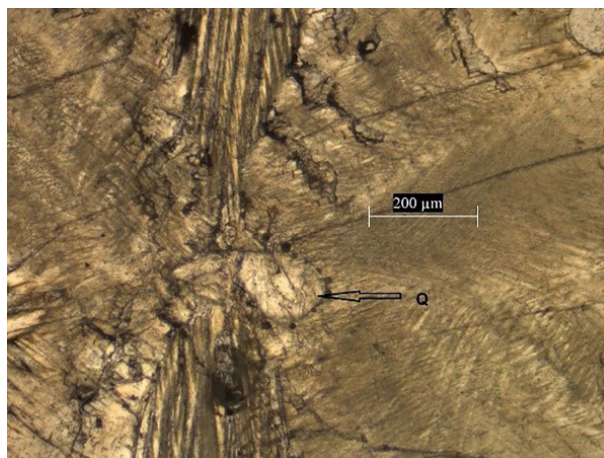


Fig. 8. Photomicrographs of sample 3: quartz crystal surrounded by diopside (parallel nicols).

texture is fine - equal grained, only in the marginal zones observe micro grained, with radial diopside. Typical spherulitic textures are not presented but features of rapid cooling - spinifex texture, very long prismatic - to needle crystals, and annealing zones attest for fast crystallization combined with high diffusion rates of components in low viscosity environment.

The diopside is the main phase and forms several aggregate types. The dominant one is the needle - like, long prismatic crystals forming spinifex texture and wavy disposition. Less common are the platy, quasi - isotropic crystals. Fluorite is the second most abundant mineral. Usually it forms spheroidal aggregates, euhedral to subhedral crystals are less common. Quartz is granular and rare. Powder diffraction analysis suggests the presence of  $\text{Zn}(\text{OH})_2$  compound with unspecified stoichiometry. The obtained Raman spectra at 155, 245, 771, 793 and 972 wavenumber ( $\text{cm}^{-1}$ ) do not specify the exact composition of zincian compound as it cannot be found precise match in the literature. The observed peaks can be interpreted as zincian dominated pigments.

The obtained experimental samples showed average values for density  $3.32 \text{ g cm}^{-3}$ , Vickers microhardness 6.3 GPa, compressive strength of 216.4 MPa and water absorption 0.14 %.

## CONCLUSIONS

Based on carbonate rocks, quartz sand, fluorite and modifying additives, polyphase materials with a

dominant diopside content were obtained from a melt in laboratory conditions. At the same time, fluorite, wollastonite, quartz, zinc hydroxide, calcite, akermanite, and chromite / chromate were registered in limited concentrations in individual experimental samples. The role of the introduced modifiers in the phase formation processes has been established.

Microscopically, diopside is found in the form of various morphological types, mainly long prismatic to needle - shaped crystals and microgranular aggregates with a comb - like, fibrous and other structure. Characteristic signs of rapid cooling and the formation of a spinifex structure have been observed. In separate zones, a transition to a gradual change from one type of structure to another has been observed. Limited areas with a glassy structure have been registered.

The presence of cavities (spherical, elliptical to irregular shape) was established, probably formed during degassing during the technological process. Fluorite aggregates (with irregular to spherical shape and low relief) were observed, partially filling cavities or localized between diopside crystals. Inclusions of fluorite, albite and other phases were found in individual diopside aggregates. The registered wollastonite forms a lamellar to layered structure and is microscopically difficult to differentiate from the diopside phase.

The applied approach allows the use of technological capabilities for forming samples from the liquid phase. The obtained experimental results represent a prerequisite for optimizing the technological regime



used, developing an additional series of compositions and a detailed technological regulation.

Based on the established mechanical parameters, phase composition and structure, the preparation of interior and exterior cladding elements for buildings is considered as a promising direction for the potential application of the synthesized materials.

### Acknowledgments

*Funding to project BG05M2OP001 - 1.002 - 0019 ensured access to diffractometer.*

**Authors' contributions:** *M.D.: Petrography, Interpretation, Writing - original draft; B.J.: Methodology, Investigation, Writing - original draft; V.P.: Conceptualization, technology; M.A.: Investigation, Writing - review and editing; G.P.: Methodology, Laboratory work. All authors: experiments and discussion.*

### REFERENCES

1. R.B. Heimann, Classic and advanced ceramics: from fundamentals to applications, John Wiley & Sons, 2010, 573.
2. W. Holland, G.H. Beall, Glass - ceramic technology, 3rd ed., Wiley - American Ceramic Society, 2019.
3. J.E. Shelby, Introduction to glass science and technology, 3rd ed., Royal Society of Chemistry, 2020.
4. E. Aydin, Problems and solutions in glass production, Society of Glass Technology, 2020.
5. S.J. Ikhmayies, Advanced ceramics, Springer Cham, 2024.
6. E. Gerasimov, A. Gerasimov, A. Atanasov, V. Toshev, D. Petkov, D. Ivanov, L. Georgieva, L. Pavlova, N. Drenska, P. Vinarov, P. Petrov, S. Buchvarov, S. Panova, S. Bagarov, S. Serbezov, S. Stefanov, S. Djambasov, T. Stoikova, T. Dackova, H. Berlinov, Technology of ceramic products and materials, S. Buchvarov (Eds.), IK Sarasvati, Sofia, 2003, (in Bulgarian).
7. R. Danzer, T. Lube, R. Damani, Ceramics science and technology, Set. Adv. Eng. Matt. 10, 4, 2008, 275-298.
8. D.W. Richerson, W.E. Lee, Modern ceramic engineering: properties, Processing and Use in Design, 4th ed., CRC press, 2018.
9. C.B. Carter, M.G. Norton, Ceramic materials: science and engineering, Springer New York, NY, 2016.
10. K.P. Misra, R.D.K. Misra (Eds.), Ceramic science and engineering, Elsevier, 2022.
11. R.A. Youness, D.M.T. Eldeen, M.A. Taha, A review on calcium silicate ceramics: properties, limitations, and solutions for their use in biomedical applications, Silicon, 15, 2023, 2493-2505.
12. S. Wu, M. Chen (Eds.), Silicate building materials SBM 2013, 1st ed., Trans Tech Publications, 2014.
13. M.B. Revuelta, Construction materials, geology, production and applications, Springer Cham, 2021, 602.
14. A.K. Chatterjee, Cement production technology, principles and practice, 1st ed., Imprint CRC Press, Boca Raton, 2018, 439.
15. C. Yang, F. Zhou, Q. Chen, G. Shi, M. Kaziana, M. Gasper, Development and application of modern building ceramic materials, Res. Applic. Mater. Sci., 5, 2, 2023, 25-32.
16. S.A.M. Abdel - Hameed, Development of wall - covering glass - ceramics from raw materials, Glass Sci. Technol., 75, 6, 2002, 290 - 293.
17. S.A.M. Abdel - Hameed, Thermal and chemical properties of diopside - wollastonite glass - ceramics in the  $\text{SiO}_2$  -  $\text{CaO}$  -  $\text{MgO}$  system from raw materials, Ceram. Int., 2003, 29, 265-269.
18. J. Feng, D. Wu, M. Long, K. Lei, Y. Sun, X. Zhao, Diopside glass - ceramics were fabricated by sintering the powder mixtures of waste glass and kaolin, Ceram. Int., 48, 2022, 27088-27096.
19. L.S. Bozadzhiev, R.L. Bozadzhiev, L.S. Doncheva, Synthetic diopside, Qualicer, 3, 2006, 89-92.
20. L.S. Bozadjiev, R.L. Bozadjiev, G.T. Georgiev, L.S. Doncheva, Diopside porcelain tile, Am. Ceram. Soc. Bull., 85, 12, 2006, 9101-9103.
21. L. Bozadjiev, L. Doncheva, Methods for diopside synthesis, J. Chem. Technol. Metall., 41, 2, 2006, 125-128.
22. R. Bozadzhiev, Wollastonite and diopside - ceramic raw materials, J. Manag. Educ., 4, 2, 2008, 205-209, (in Bulgarian).
23. R. Titorenkova, T. Dimitrov, Y. Tzvetanova, Synthesis and characterization of Cr - doped diopside ceramics, Rev. Bul. Geol. Soc., 83, 3,

- 2022, 47-50.
24. B.N. Sherikar, B. Sahoo, A.M. Umarji, One - step synthesis of diopside ( $\text{CaMgSi}_2\text{O}_6$ ) ceramic powder by solution combustion method, *Adv. Powder Technol.*, 31, 8, 2020, 3492-3499.
25. R. Titorenkova, V. Kostov-Kytin, Ts. Dimitrov, Synthesis, phase composition and characterization of Co - diopside ceramic pigments, *Ceram. Int.*, 48, 24, 2022, 36781-36788.
26. T. Dimitrov, R. Titorenkova, O. Petrov, Diopside ceramic pigments obtained by a sol - gel method with the participation of different chromophore elements, *Proceedings of University of Ruse Angel Kanchev*, 61, 10.1., ISSN: 2603 - 4123, 2022, 74-79.